Available online at www.sciencedirect.com
ScienceDirect
Trans. Nonferrous Met. Soc. China 20(2010) s862−s867
Transactions of Nonferrous Metals Society of China
www.tnmsc.cn

Microstructure and mechanical properties of rheo-diecasting AZ91D Mg alloy

YANG Liu-qing(杨柳青)[1,2], KANG Yong-lin(康永林)[2], ZHANG Fan(张 帆)[2], XU Jun(徐 骏)[1]

1. General Research Institute for Nonferrous Metals, Beijing 100088, China;
2. School of Materials Science and Engineering, University of Science and Technology Beijing, Beijing 100083, China

Received 15 May 2010; accepted 25 June 2010

Abstract: Taking AZ91D magnesium alloy as experimental material, the rheo-diecasting process was implemented by combining the self-developed taper barrel rheomoulding(TBR) machine with high pressure die casting(HPDC) machine. Microstructural characteristics of the rheo-diecasting components were investigated in different processing parameters. Microstructural evolution and solidification behavior of the semisolid slurry during the rheo-diecasting process were discussed, and tensile properties of the components were studied as well. The results show that, with the rotation speed of the internal taper barrel increasing, the microstructure of the components becomes fine with solid particles nearly spherical and uniformly distributed on the matrix. When the rotation speed is 700 r/min, the primary α-Mg particles have an average size of about 45 μm and a shape factor of about 0.81; the primary α-Mg particles become round and homogeneous with shearing temperature increasing, but the average size is slightly larger. The solidification of the alloy melt during the rheo-diecasting process is composed of two distinct stages: the primary solidification and the secondary solidification. Compared with the conventional die-casting process, the rheo-diecasting process would improve the tensile properties of the components, especially the elongation by 80%.

Key words: AZ91D magnesium alloy; rheo-diecasting; microstructural characteristics; tensile properties

1 Introduction

Due to the widespread applications and applicability to many processing methods, shorter process, compact casting structure and high precision, rheoforming has received attention from many scholars who carried out a great deal of work on theories, experiments, techniques and equipment developments and made rapid progress, which made rheoforming a new focus in semisolid metal processing field[1−2]. Combining semisolid slurry preparation technology with die-casting technology develops the rheo-diecasting process, which keeps not only the characteristics of rheoforming but also the high efficiency and low cost of die-casting, and it assuredly has great industrial application prospect[3−5]. The representative rheo-diecasting process mainly includes the twin-screw rheomoulding process exploited by FAN et al[6−7], but so far this technology has not achieved large-scale industrial application.

In this work, combining the self-developed taper barrel rheomoulding(TBR) machine with TOYO BD-900V4-T high pressure die casting(HPDC) machine, the integrated rheo-diecasting process from semisolid slurry preparation to die-casting was successfully realized, and the widely applied AZ91D magnesium alloy was used as experimental material. Microstructural characteristics of therheo diecasting components were investigated in different processing parameters. The microstructural evolution and solidification behavior of the semisolid slurry during the rheo-diecasting process were discussed, and the tensile properties of the components were studied as well.

2 Experimental

2.1 Experimental device and materials

The main experimental device is the self-developed TBR machine. It consists of a semisolid preparing device, a driving system, an elevating system, a semisolid conveying appliance, a gas protection system, and a temperature control system[8]. The experimental die-casting device is TOYO BD-900V4-T HPDC machine, and the die-casting moulds are selected from architectural scraper mould and mechanical property mould. The experimental material is commercial high-purity AZ91D magnesium alloy ingot (provided by Beijing Guangling Jinghua Science and Technology Co.,

Foundation Item: Project (2009DFB50210) supported by the International S&T Cooperation Program of China; Project (2006CB605203) supported by the National Basic Research Program of China
Corresponding author: YANG Liu-qing; Tel: +86-10-82241229; E-mail: ylqylq1999@yahoo.com.cn

Ltd). Liquidus and solidus of the alloy are 595 ˚C and 470 ˚C, respectively. The magnesium ingot was tested by ARL3460 direct reading spectrometer and Table 1 presents its chemical composition.

Table 1 Chemical composition of AZ91D magnesium alloy ingot (mass fraction, %)

Al	Zn	Mn	Si	Fe
9.4453	0.6616	0.2043	0.0363	0.0009
Cu	Ni	Be	Mg	
0.0047	0.0010	0.0007	bal.	

2.2 Experimental procedure

The AZ91D ingot was put into a preheating furnace whose preheating temperature was 150 ˚C for 1 h, then it was conveyed to a melting furnace till the temperature reached 680 ˚C and the ingot melted. Use the covering flux of magnesium alloy during the melting process to protect the alloy melt from oxidative burning. Pour the liquid alloy into TBR machine whose parameters were set specifically in advance. While passing the taper barrel gap, the melt experienced intense shearing during solidification because of the shear stress field caused by relatively high-speed rotation of taper barrel, and the shearing time was 5–8 s. Finally, the prepared semisolid slurry was transferred into TOYO BD-900V4-T HPDC machine via slurry conveying appliance to carry on die-casting. Both the semisolid slurry preparing and conveying were carried out in a closed environment and Ar was applied to defend the magnesium alloy melt against oxidative burning. The die-casting processing parameters in the experiment were as follows: clamp force 9 000 kN, casting pressure 75 MPa, low speed 0.35 m/s, high speed 3.5 m/s and mould temperature 200 ˚C.

The samples were cutting from the sprue of the architectural scrape, followed by rough grinding, fine grinding and polishing. The polished samples were then etched by 4% (volume fraction)nitric acid alcohol and flushed with hot water and finally blew dry. A NEOPHOT 21 optical microscope and a Cambridge S-360 scanning electron microscope were utilized for microstructural observation and analysis. The tensile test was carried out on MTS810 material testing machine referring to GB/T 228-2002, and the strain rate was 1.0 mm/min. Fig.1 is the photograph of the rheo-diecasting component for mechanical properties test. The influence of processing parameters on mean size and shape factor of primary α-Mg particles was investigated using Image Tool 3.0 image analysis software. The primary α-Mg particle diameter is symbolized by the equivalent area diameter

$$D_{eq}=(\sum_{N=1}^{N}\sqrt{4A_N/\pi})/N \quad (1)$$

and the shape factor is recorded as

$$F=(\sum_{N=1}^{N}4\pi A_N/P_N^2)/N \quad (2)$$

where A_N and P_N are the area and perimeter of the Nth primary α-Mg particle, respectively, and N is the number of particles. Therefore, the primary α-Mg particles will be homogeneous and round when F is close to 1[9−10].

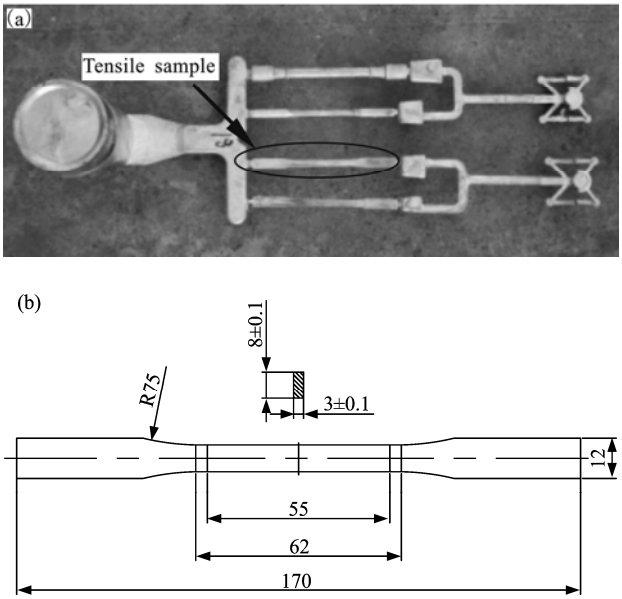

Fig.1 Photograph of rheo-diecasting component for mechanical property test(a) and size of tensile sample(b)(unit:mm)

3 Results and discussion

3.1 Microstructural characteristics

Fig.2 shows the microstructure of the rheo-diecasting architectural scraper at different locations, when pouring temperature is 680 ˚C, rotation speed of internal taper barrel is 600 r/min, shearing temperature is 590 ˚C and the taper barrel gap is 3 mm. It can be seen that the microstructure of the rheo-diecasting component is mainly composed of fine granular and nearly spherical primary α-Mg particles, and there are few small pores and no dendrites, indicating that the process can get the rheo-diecasting components with typical semisolid features. Primary α-Mg particles at position *A* are coarse and granular or nearly spherical. Compared with position *A*, the microstructure at position *B* is fine and round, consisting of spherical primary solid particles. Primary α-Mg particles become finer but non-uniform at position *C*. At positions *D*, *E*, and *F*, it can be seen that the microstructure microstructure is not obviously changed and is similar to the microstructure of position *C*, except that the distribution and the size of primary α-Mg particles are more uneven and there are a few pores. The changing of microstructure at different positions of the

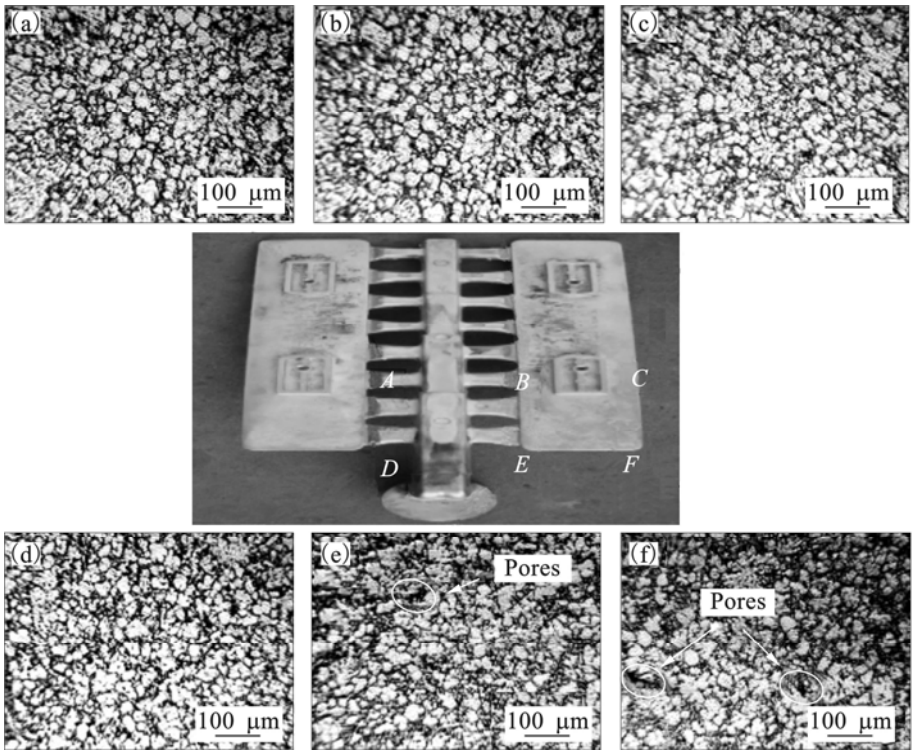

Fig.2 Microstructures of rheo-diecasting architectural scraper: (a) Position *A*; (b) Position *B*; (c) Position *C*; (d) Position *D*; (e) Position *E*; (f) Position *F*

architectural scraper indicates that the solidification of semisolid slurry during rheo-diecasting is influenced by the preparation process of slurry, the die-casting process and mould structure, and so on.

Fig.3 shows the effects of rotation speed on mean particle diameter and shape factor, when pouring temperature is 680 ˚C, shearing temperature is 590 ˚C and the taper barrel gap is 3 mm. It can be seen that, when rotation speed is 300 r/min, the mean size of primary α-Mg particles is 63 μm and the shape factor is 0.46, and the morphology is not so round; when rotation speed is 500 r/min, the mean size is about 54 μm and shape factor is 0.62; as rotation speed reaches 600 r/min, the primary α-Mg particle diameter is 46 μm and the shape factor is 0.78; compared with that of 600 r/min, the mean size and shape factor of the primary particles at 700 r/min do not change too much. In the semisolid slurry preparation process, intense shear stress field not only makes the temperature field and concentration field of undercooled melt homogeneous, but also results in morphological changes of primary α-Mg particles from dendrite to spherical via rosette. Increasing intensity of the shear stress field (rotation speed) tremendously will make primary α-Mg particles finer, rounder and more homogeneous[11].

Fig.4 shows the effects of shearing temperature on mean particle diameter and shape factor. When the shearing temperature is 600 ˚C, the primary α-Mg particle

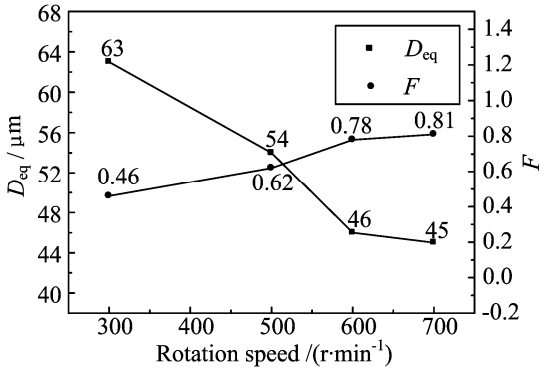

Fig.3 Effects of rotation speed on mean particle diameter and shape factor

diameter is about 44 μm, the shaper factor is 0.75 and the solid fraction is 43%; when the shearing temperature is 580 ˚C, the microstructural morphology is composed of spherical and nearly spherical primary α-Mg particles, which distribute uniformly on the matrix, the shape factor is 0.82, the mean particle diameter is 47 μm and the solid fraction is 56%. As shearing temperature decreases to 570 ˚C, the primary α-Mg particles will become rounder and more homogeneous. Compared with that at 580 ˚C, the mean diameter at 570 ˚C is larger, and the solid fraction is higher, about 64%. Based on above analysis, during the semisolid slurry preparation, cooling rate of the alloy melt at lower than 600 ˚C is relative small in the taper barrel gap, and the effective shearing time is short, which results in that free crystals in the semisolid slurry are

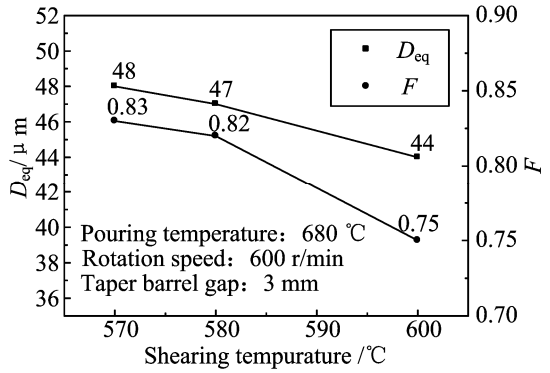

Fig.4 Effects of shearing temperature on mean particle diameter and shape factor

fewer and have no regular shape. Such slurry is quenched by the die-casting mould, but there is no enough time for free crystals to grow, resulting in fine and out-of-round primary α-Mg particles. But when the shearing temperature is 570 ˚C, the cooling intensity of the melt in the gap is stronger, and the melt has higher nucleation rate, meanwhile, the effective shearing time is longer, which helps to prepare relative large and round primary α-Mg particles with high solid fraction. In the following rheo-diecasting process, the microstructure of architectural scraper inherits such features, but low shearing temperature will degenerate the fluidity of semisolid slurry and increase difficulty in the following slurry conveying and rheo-diecasting process, so choosing proper shearing temperature is of great importance.

3.2 Microstructural evolution and solidification behavior

Based on the rheo-diecasting process and experimental analysis in this work, it can be seen that the solidification of alloy melt generally experiences two stages: the primary solidification and the secondary solidification. The former mainly occurs in the semisolid slurry preparation process, including continuous fast cooling, isothermal shearing and fast conveying of the semisolid slurry, wherein the continuous fast cooling exists when the melt enters the taper barrel gap. The melt flow in the gap is finished under comprehensive effect of the cooling of the taper barrels, intense shearing turbulence of the internal barrel and self-stirring of the melt. Because of the strong cooling effect of internal and external taper barrel on the alloy melt, the temperature of the melt with a certain superheating decreasing to a given solidification temperature in a short time. Meanwhile, the intense turbulence of internal taper barrel makes concentration field relatively homogeneous and temperature field inside the semisolid slurry, forming lots of effective nucleation sites, which will become nucleus ultimately as the temperature of the melt decreases. When the temperature of the melt gradually decreases to be the same as that of taper barrels, the alloy melt begins isothermal shearing where intense turbulence improves the heat-transfer and mass-transfer process and suppressing growth of the particles. GUO et al [12−13] think that the spherical particles will self-rotate as they grow, and make distribution of solute and temperature more uniform, which benefits to spheroidization of the particles. Finally, the semisolid slurry with spherical or nearly spherical characteristics is prepared. Based on growth kinetics, the condition for granular particles to grow spherically is described as [14]:

$$R_\Gamma = \left[6+15\left(1+\frac{\lambda_s}{\lambda_l}\right)\right]R^* \tag{3}$$

where R_Γ is the critical radius of granular particles growing in spherical means. λ_s and λ_l are the thermal conductivity of solid and liquid alloy, respectively and R^* is the critical radius of granular particles. Besides, a part of nuclei in the undercooling melt distribute on the wall of the taper barrels and grow as dendrites, which will be sheared and stirred by the internal taper barrel, resulting in the primary dendrites fragmenting and dissociating into the melt. Because of the uniform concentration field and temperature field in the alloy melt, preferred growth does not occur to the dissociative dendrites. Furthermore, surface energy has an effect on the dissociative dendrites and makes them grow in the direction of shrinking surface area to become spherical. The above stage is the key part for particle growth and spheroidization, which determines the final microstructural characteristics. During the following slurry conveying, the primary α-Mg particles grow and spheroidize further. In a perspective of solidification morphology, particle spheroidization, is the result of solid-liquid interface change substantially during the transformation of steady-state to non-steady and the steady-state maintaining course. In brief, under pure diffusion conditions, steadiness of the solid-liquid interface can be described as the classic M-S theory [15−16]:

$$S(\omega) = -T_m \Gamma \omega^2 - G_L + mG_C \frac{\omega^* - (v/D)}{\omega^* - (v/D)(1-k_0)} \tag{4}$$

where T_m is the alloy melting point; Γ is the surface tension constant; m is the liquidus slope; ω is the vibration frequency; ω^* is the fluctuation frequency of medium along the solid-liquid interface; G_L and G_C are the temperature gradient and concentration gradient when $\delta = 0$, respectively. Positive or negative of $S(\omega)$ corresponds to the growth or decay of interference amplitude, and decides the steadiness of solid-liquid interface. The classic M-S theory is based on single

particle, that is, the growth of one particle is not influenced by others. However, in TBR process the primary α-Mg particles have a high grain density and a short grain distance, and the composition field of one particle would stack on that of adjacent particles, which makes the concentration gradient decline around each particle and further results in the decreasing of the destabilizing effect caused by concentration gradient. Therefore, high particle density is beneficial to the steadiness of solid-liquid interface and keeping the particles growing spherically.

Secondary solidification mainly occurs when the slurry enters the cold chamber, the die-casting cavity and mold filling. Due to high cooling rate of the slurry by the injection chamber and die-casting cavity, remaining liquid is subjected to rapid solidification in the cavity of the HPDC machine. Meanwhile, the prepared semisolid slurry is affected by the intense shear stress field, temperature and concentration distribute uniformly inside the remaining liquid, and then the "big bang" nucleation will happen inside. Different from the primary solidification, remaining liquid in the secondary solidification has high cooling rate (in the order of 10^3 ˚C/s[6]), so the nuclei do not have any chance to grow, resulting in homogeneous and fine secondary microstructure finally[7,17]. Fig.5 presents the typical micrograph of the architectural scrape obtained under such processing conditions: pouring temperature 680 ˚C, shearing temperature 590 ˚C, taper barrel gap 3 mm and rotation speed 600 r/min. In Fig.5(a), the big white particles are primary α_1(Mg), and the fine white particles in the dark grey region are secondary α_2 (Mg). In Fig.5(b), the big spherical grey particles are primary α_1 (Mg), and the fine out-of-shape particles are secondary α_2 (Mg). The white reticular phase along boundaries of the primary phase is the β-$Mg_{17}Al_{12}$ divorced eutectic resulted from non-equilibrium solidification, and the black phase around β phase is the secondary β-$Mg_{17}Al_{12}$ phase precipitation from primary α_1(Mg).

3.3 Tensile properties

Table 2 summarizes the tensile properties of AZ91D magnesium tensile samples under different processes. In contrast to thixocasting, the ultimate tensile strength (UTS) of the tensile samples by TBR process preparation is high, and both the yield strength(YS) and the elongation rise. Compared with the twin-screw rheomoulding techniques, the samples have low UTS and elongation, but the YS does not change too much. Conventional die-casting was performed to compare with the rheo-diecasting tensile samples by using the same HPDC machine and die-casting mould. The results show that the YS of the samples is roughly the same as conventional die-casting, while UTS and elongation of the former increase, especially the elongation is improved by 80%.

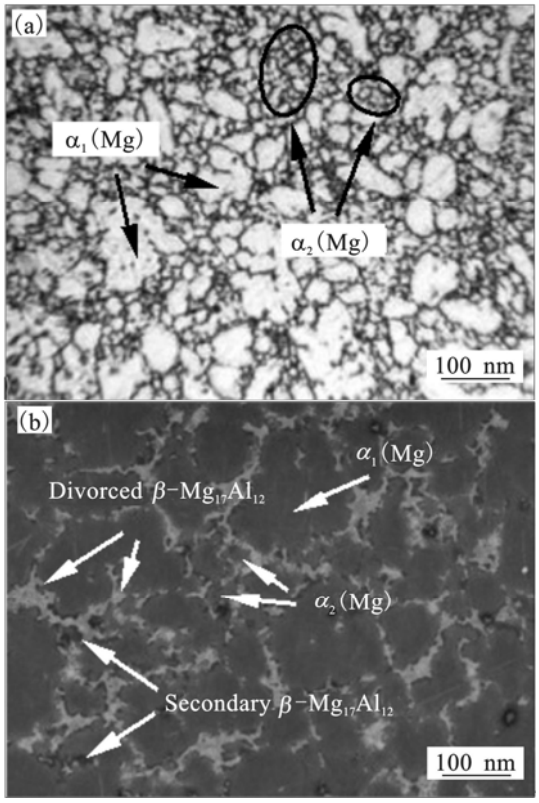

Fig.5 Typical micrographs of rheo-diecasting architectural scrape: (a) Optical micrograph; (b) SEM micrograph

Table 2 Tensile properties of AZ91D magnesium tensile samples in different processes

Process	YS/ MPa	UTS/ MPa	Elongation/ %
Thixocasting[18]	134	223	3.6
Rheo-diecasing (Twin-screw rheomoulding process)[6]	145	248	7.4
Rheo-diecasing(TBR process)	138	225	4.5
HPDC	144	200	2.5

Factors that result in the degeneration of tensile properties in die-casting process mainly include internal porosity, micro-shrinkage, hot crack, microstructural non-uniformity and so on. In conventional die-casting process, due to high pouring temperature, the coarse dendrite and micro-shrinkage or shrinkage would form during the solidification in the die-casting mold cavity, which leads to microstructural non-uniformity and inferior compactness inside the components and worsens the tensile properties. In rheo-diecasting process, the pouring temperature is not high, moreover the melt

experiences intense shearing and stirring before pouring, which is beneficial to uniform structure and high compactness, with the result that the tensile strength and elongation rise. The reasons that the tensile properties of the rheo-diecasting parts are inferior to that of the twin-screw rheomoulding process may attribute to the short shearing time and low shearing rate, and that result in microstructural non-uniformity. It is believed that mechanical properties of die-casing components have a strong dependence on microstructural morphology[19]. The unique microstructure feature that primary α-Mg globules uniformly distributed on the matrix may help the components obtain good mechanical properties.

4 Conclusions

1) The self-developed taper barrel rheomoulding (TBR) machine was introduced. Combining with HPDC machine, the integrated rheo-diecasting process from semisolid slurry preparation to die-casting was implemented. The rheo-diecasting process is able to obtain the components in which primary α-Mg particles are fine, nearly spherical and uniformly distributed on the matrix.

2) With the rotation speed increasing, the microstructure of the rheo-diecasting components becomes fine and the solid particles nearly spherical; when shearing temperature is lower, the components will have a better microstructural morphology, the primary α-Mg particles tends to be round and uniformly distribute on the matrix, but low shearing temperature will not be beneficial to the flowing of the semisolid slurry, and subsequently will affect on slurry conveying. The solidification of AZ91D magnesium alloy melt taking place during the rheo-diecasting process is composed of two distinct stages: the primary solidification and the secondary solidification.

3) Compared with conventional die-casting process, the rheo-diecasting process successfully improves tensile properties of the components, especially the elongation improved by 80%. But more experiments should be taken to improve and optimize the rheo-diecasting process.

References

[1] KANG Yong-lin, MAO Wei-min, HU Zhuang-qi. Theory and technology of semisolid metal forming processing[M]. Beijing: Science Press, 2004. (In Chinese).

[2] FLEMINGS M C. Behavior of metal alloys in the semisolid state[J]. Metallurgical Transactions B, 1991, 22B:269−293.

[3] YANG Liu-qing, KANG Yong-lin, ZHANG Fan, TAO Tao. Study on rheo-diecasting process and properties of AZ91HP magnesium Alloy[J]. Foundry, 2009, 58(11): 1119−1122. (In Chinese).

[4] YANG Liu-qing, KANG Yong-lin, ZHANG Fan, TAO Tao. Study on rheo-diecasting process and properties of AZ91HP magnesium Alloy[J]. Foundry, 2009, 58(11): 1119−1122. (In Chinese).

[5] JI Lian-qing, XIONG Shou-mei, MASAYUKI M, YOSHIHIDE M, SHINGO I. Effects of casting pressure on microstructure and mechanical properties of super slow speed die castings of ADC12 aluminum alloy[J]. Foundry, 2007, 56(11): 1167−1170. (In Chinese).

[6] FAN Z. Development of the rheo-diecasting process for magnesium alloys[J]. Materials Science and Engineering A, 2005, 413/414: 72−78.

[7] JI S, FAN Z, BEVIS M J. Semisolid processing of engineering alloys by a twin-screw rheomoulding process[J]. Materials Science and Engineering A, 2001, 299: 210−217.

[8] KANG Yong-lin, YANG Liu-qing, SONG Ren-bo, ZHANG Fan, TAO Tao. Study on microstructure-processing relationship of a semisolid rheocasting A357 aluminum alloy[J]. Solid State Phenomena, 2008, 141/142/143: 157−162.

[9] TZIMAS E, ZAVALIANGOS A. A comparative characterization of near-equiaxed microstructures as produced by spray casting, magnetohydrodynamic casting and the stress induced, melt activated process[J]. Materials Science and Engineering A, 2000, 289: 217−227.

[10] LIU Zheng, MAO Wei-min, ZHAO Zhen-duo. Semisolid A356 alloy slurry prepared by a new process[J]. Acta Metallurgica Sinica, 2009, 45(4): 507−512. (In Chinese).

[11] XU Yue, KANG Yong-lin, WANG Zhao-hui, DONG Wen-chao, LIU Jin-wei. Preparation of semisolid slurry of AZ91D Mg alloy[J]. Special Casting and Nonferrous Alloys, 2004(5):12−14. (In Chinese).

[12] GUO Hong-min,YANG Xiang-jie, LUO Xue-quan. Formation of grain refined and non-dendritic microstructure of an aluminum alloy under angular oscillation[J]. Journal of Alloys and Compounds, 2009, 482: 412−415.

[13] GUAN Ren-guo, WEN Jing-lin, WANG Shun-cheng, LIU Xiang-hua. Microstructure behavior and metal flow during continuously extending-extrusion forming of semisolid A2017 alloy[J]. Transactions of Nonferrous Metals Society of China, 2006, 16: 382−386.

[14] GUAN Ren-guo, MA Wei-min. Theory and technology of semisolid metal forming[M]. Beijing: Metallurgical Industry Press, 2005. (In Chinese) .

[15] TRIVEDI R. Morphological stability of a solid particle growing from a binary alloy melt[J]. Journal of Crystal Growth, 1980, 48: 93−99

[16] HU Han-qi. Principles of metal solidification[M]. Beijing: China Machine Press, 2000. (In Chinese) .

[17] FAN Z, LIU G. Solidification behaviour of AZ91D alloy under intensive forced convection in the RDC process[J]. Acta Materialia, 2005, 53: 4345−4357.

[18] CZERWINSKI F, ZIELINSKA-LIPIEC A, PINET P J, OVERBEEKE J. Correlating the microstructure and tensile properties of a thixomolded AZ91D magnesium alloy[J]. Acta Materialia, 2001, 49:1225−1235.

[19] DU X H, ZHANG E L. Microstructure and mechanical behaviour of semisolid die-casting AZ91D magnesium alloy[J]. Materials Letter, 2007, 61: 2333−2337.

(Edited by LIU Hua-sen)